Energy-stress-mediated activation of AMPK sensitizes MPS1 kinase inhibition in triple-negative breast cancer

JONG SEUNG LIM[1,2], EUNKYOUNG KIM[1,3], JIN-SOOK SONG[1] and SUNJOO AHN[1,3]

[1]Therapeutics & Biotechnology Division, Korea Research Institute of Chemical Technology, Daejeon 34114, Republic of Korea; [2]School of Pharmacy, Sungkyunkwan University, Suwon 16419, Republic of Korea; [3]Department of Medicinal Chemistry and Pharmacology, University of Science and Technology, Daejeon 34113, Republic of Korea

Received November 23, 2023; Accepted April 26, 2024

DOI: 10.3892/or.2024.8760

Abstract. Monopolar spindle 1 kinase (Mps1, also known as TTK protein kinase) inhibitors exert marked anticancer effects against triple-negative breast cancer (TNBC) by causing genomic instability and cell death. As aneuploid cells are vulnerable to compounds that induce energy stress through adenosine monophosphate-activated protein kinase (AMPK) activation, the synergistic effect of Mps1/TTK inhibition and AMPK activation was investigated in the present study. The combined effects of CFI-402257, an Mps1/TTK inhibitor, and AICAR, an AMPK agonist, were evaluated in terms of cytotoxicity, cell-cycle distribution, and *in vivo* xenograft models. Additional molecular mechanistic studies were conducted to elucidate the mechanisms underlying apoptosis and autophagic cell death. The combination of CFI-402257 and AICAR showed selective cytotoxicity in a TNBC cell line. The formation of polyploid cells was attenuated, and apoptosis was increased by the combination treatment, which also induced autophagy through dual inhibition of the PI3K/Akt/mTOR and mitogen-activated protein kinase (MAPK) signaling pathways. Additionally, the combination therapy showed strongly improved efficacy in comparison with CFI-402257 and AICAR monotherapy in the MDA-MB-231 xenograft model. The present study suggested that the combination of CFI-402257 and AICAR is a promising therapeutic strategy for TNBC.

Correspondence to: Dr Sunjoo Ahn, Therapeutics & Biotechnology Division, Korea Research Institute of Chemical Technology, 141 Gajeong-ro, Yuseong, Daejeon 34114, Republic of Korea
E-mail: sahn@krict.re.kr

Abbreviations: AMP, adenosine monophosphate; AMPK, AMP-activated protein kinase; ATP, adenosine triphosphate; ER, estrogen receptor; HMEC, human mammary epithelial cells; Mps1, monopolar spindle 1 kinase; PR, progesterone receptor; SAC, spindle assembly complex; TNBC, triple-negative breast cancer

Key words: breast cancer, TNBC, AMPK, MPS1 kinase, TTK protein kinase, energy stress

Introduction

Breast cancer (BC) is a common form of cancer in women, and its incidence and mortality have been increasing (1). BC is categorized into four molecular subtypes based on the presence of the estrogen receptor (ER), progesterone receptor (PR), Ki67 and human epidermal growth factor receptor 2 (HER2): Luminal A (ER^+, PR^+, $HER2^-$, $Ki67^-$), luminal B (ER^+, PR^+, $HER2^{-/+}$, $Ki67^+$), HER2 overexpressing (ER^-, PR^-, $HER2^+$) and triple-negative (ER^-, PR^-, $HER2^-$) (2). Among these subtypes, triple-negative BC (TNBC) accounts for 12-17% of all BCs and shows features, such as aggressive disease with dismal outcomes, absence of a therapeutic target for decades, heterogeneous disease and higher incidence in the younger age group (3). Although conventional chemotherapy can achieve a response in patients with TNBC, the risk of recurrence is higher than that in other types of BC. Additionally, the adverse effects of conventional chemotherapy can be difficult to overcome, highlighting an urgent need to identify novel therapeutic options for TNBC (4).

Numerous mammalian cell divisions are regulated by cell-cycle checkpoint proteins. In cancer cells, these checkpoint proteins are mostly overexpressed or mutated and could be potential targets for cancer therapies (5). The spindle assembly complex (SAC; also known as the mitotic checkpoint) is a signaling pathway that plays a role in monitoring daughter chromatid separation and arrests mitosis if the chromatid is separated incorrectly (6). In the SAC, monopolar spindle 1 kinase (Mps1) is the core protein that recruits SAC-related proteins and is activated in unattached kinetochores. Inhibition of Mps1/TTK causes abrogation of the mitotic checkpoint complex and anaphase-promoting complex, thereby inducing immature mitosis in cancer cells. This results in massive aneuploidy and cell death due to mitotic catastrophe (7,8). Mps1/TTK is overexpressed in some cancer cells that have a poor prognosis, especially in TNBC (9-12). Thus, the inhibition of Mps1/TTK can be a promising target for TNBC therapy. Several Mps1/TTK inhibitors are under investigation in clinical trials to treat solid cancers, and efforts are underway to overcome hematologic and gastrointestinal

toxicities (13,14). Various combination strategies were tried to enhance therapeutic index of Mps1/TTK inhibitors by reducing their doses (15,16). Based on the synergic preclinical efficacy, most of Mps1/TTK inhibitors undergoing clinical trials have been studied in combination with paclitaxel (17). CFI-402257 combined with weekly paclitaxel was well tolerated during a Phase 1b trial [Philippe Bedard, Mihaela Mates, John Hilton, *et al*: Abstract P3-07-10: CCTG IND.236: A Phase 1b trial of combined CFI-402257 and weekly paclitaxel in patients with HER2-negative ($HER2^-$) advanced BC. Cancer Res (2023) 83 (5_Supplement): P3-07-10]. However, considerable toxicity was observed in the combination of BAY 1217389 with paclitaxel without a therapeutic window (18). Therefore, novel combination approach with alternative drugs rather than paclitaxel with Mps1/TTK inhibitors would be meaningful.

Adenosine monophosphate (AMP)-activated protein kinase (AMPK) is a cellular energy stress sensor that is activated by the AMP: Adenosine triphosphate (ATP) ratio in the cytoplasm (19). Aneuploid cells are sensitive to energy- and proteotoxic stress-inducing compounds, including AMPK activators. Aneuploidy plays a dual role in tumorigenesis and is a potential therapeutic vulnerability in cancer. The antineoplastic activity of AMPK activators is more effective in high-grade aneuploidy than in low-grade aneuploidy (20,21). Moreover, the p-AMPK level in patients with TNBC is ~90% lower than that in healthy patients and related to a higher grade of cancer (22,23). Therefore, the anticancer effects of AMPK agonists on the excessive aneuploidy, induced by MPS1/TTK inhibitors in TNBC, were investigated.

In the present study, it was sought to evaluate the synergistic effect of the combination strategy of Mps1/TTK inhibitors with AMPK agonist in order to increase therapeutic range through dose reduction. Based on understanding the mechanisms underlying the effects of the combination of CFI-402257 and AICAR, combining Mps1/TTK inhibitors with AMPK agonists appears to be a rational option for BC.

Materials and methods

Ethics statement. All applicable national and institutional guidelines for the care and use of animals were followed. The protocols for animal experiments were approved (approval no. 2021-7F-08-02; approval date: 2022-08-27) by the Animal Ethics Committee of the Korea Research Institute of Chemical Technology (Daejeon, Korea). The study was conducted in compliance with the ARRIVE guidelines.

Chemicals and reagents. CFI-402257, empesertib and BOS-175722 were purchased from MedChemExpress. AICAR was purchased from Cayman Chemical Company. A-23187, metformin and nocodazole were provided from Sigma-Aldrich; Merck KGaA. The primary antibodies for phosphorylated (p-) TTK (cat. no. 44-1325G; RRID: AB_2533594; Thermo Fisher Scientific, Inc.), Cyclin B1 (cat. no. sc-7393; RRID: AB_627336), Cyclin D1 (cat. no. sc-8396; RRID: AB_627344), Cyclin E (cat. no. sc-248; RRID: AB_627362) and p27 (cat. no. sc-1641; RRID: AB_628074; all from Santa Cruz Biotechnology, Inc.) were used. The following primary antibodies were obtained from Cell Signaling Technology, Inc.: TTK (cat. no. 5469; RRID: AB_10.692670), p-AMPK (cat. no. 2535; RRID: AB_331250), AMPK (cat. no. 2532; RRID: AB_33033198), p-cdc2 (cat. no. 9111; RRID: AB_331460), CDK2 (cat. no. 2546; RRID: AB_2276129), cleaved caspase-3 (cat. no. 9661; RRID: AB_234188), cleaved PARP (cat. no. 5625; RRID: AB_10699459), LC3B (cat. no. 2775; RRID: AB_915950), beclin-1 (cat. no. 3738; RRID: AB_490837), Atg3 (cat. no. 3415; RRID: AB_2059244), Atg7 (cat. no. 8558; RRID: AB_10831194), p-PI3K (cat. no. 4228; RRID: AB_659940), PI3K (cat. no. 4292; RRID: AB_329869), p-Akt (cat. no. 9271; RRID: AB_329825), p-mTOR (cat. no. 2971; RRID: AB_330970), mTOR (cat. no. 2983; RRID: AB_2105622), ERK (cat. no. 9102; RRID: AB_330744), p-p38 (cat. no. 9211; RRID: AB_331641) and p38 (cat. no. 9212; RRID: AB_330713). The secondary antibodies were purchased from Novus Biologicals, LLC (cat. no. NB7561) and GeneTex (cat. no. GTX213110-01) respectively. Phenol Red-free Matrigel was purchased from Corning, Inc. (cat. no. 356237).

Cell culture. Human mammary epithelial cells (HMEC; cat. no. CC-2551) were obtained from Lonza Group, Ltd. and incubated in MEBM™ basal medium (cat. no. CC-3151) and MEGM™ SingleQuits™ supplements (cat. no. CC-4136). MCF-7 (cat. no. HTB-22) and MDA-MB-231 (cat. no. CRM-HTB-26) were obtained from the American Type Culture Collection and incubated in RPMI-1640 medium (cat. no. SH30027.01; Hyclone; Cytiva) containing 10% fetal bovine serum (cat. no. SH030919.03; Hyclone; Cytiva) and 1% penicillin/streptomycin at 37˚C in a 5% CO_2 incubator. All cell lines were tested negative for mycoplasma contamination using a MycoAlert® Mycoplasma Detection Kit (Lonza Group, Ltd.).

Cytotoxicity assay. Cell viability was measured using Cyto X reagent (cat. no. CYT1000; LPS Solution; https://lpss.co.kr). Cells were seeded at a density of $2x10^3$ cells per well (MCF-7 and MDA-MB-231) and $4x10^3$ cells per well (HMECs) in a 96-well plate. After 24 h, treatment with 0-1,000 nM CFI-402257, Empesertib and BOS-172722, 0-1,200 μM AICAR, 0-10 μM A-23187 and 100 mM metformin was conducted according to the experimental conditions. After 72 and 120 h of incubation, 10-μl Cyto X reagent (LPS solution) was added and incubated at 37˚C in a 5% CO_2 incubator for an additional 2 h. Thereafter, the absorbance was detected on a spectrophotometer (BioTek; Agilent Technologies, Inc.), and the IC_{50} values for each compound were determined using GraphPad Prism 8 (Dotmatics), including logarithmic transformation, normalization and non-linear regression (RRID: SCR_002798).

Cell-cycle distribution analysis. MDA-MB-231 cells were seeded at a density of $1x10^5$ in 6-well plates. After 24 h of incubation, the cells were treated with CFI-402257 (100 nM), AICAR (300 μM), or a combination of both for 72 h. The total number of cells ($1x10^6$ cells) were harvested and washed. Subsequently, the cells were fixed in 70% ice-cold ethanol at -20˚C for at least 3 h prior to staining. Cells were stained with 200 μl of Muse® Cell Cycle Reagent (cat. no. 4700-1495; Merck KGaA) and incubated for 30 min at 20-25˚C in the dark. Data were analyzed using a Muse® Cell Analyzer (software version 1.5; Merck KGaA). All procedures were conducted according to the manufacturer's instructions.

Annexin V apoptosis assay. A total of $1x10^5$ of MDA-MB-231 cells in 6-well plates were cultured with CFI-402257 (100 nM), AICAR (300 μM), or a combination of both. After 72 h, the suspended and adherent cells were harvested and washed with Dulbecco's Phosphate Buffered Saline (DPBS). After washing, each tube was stained with 100 μl of the Muse® Annexin V & Dead Cell reagent (cat. no. MCH100105; Merck KGaA) and incubated for 20 min at room temperature in the dark. Samples were prepared and stained according to the manufacturer's protocol and analyzed using a Muse® Cell Analyzer (software version 1.5; Merck KGaA).

Acridine orange (AO) staining. AO stain, a cell-permeable reagent, conjugates with nuclear acid. When it combines with DNA, the green signal appears; however, a red signal appears in an acidic environment, such as an autophagosome. MDA-MB-231 cells were seeded in 35-mm confocal dishes. After 24 h, the cells were treated with CFI-402257 (100 nM), AICAR (300 μM), or a combination of the two for 72 h. Thereafter, the cells were stained with 1 μg/ml of AO (cat. no. A8097; Sigma-Aldrich; Merck KGaA) for 20 min at room temperature in the dark. Images were obtained using an inverted fluorescence phase-contrast microscope (K1-Fluo; Nanoscope Systems, Inc.).

Western blot analysis. The cells were trypsinized and rinsed with cold DPBS. Cells were then lysed on ice using RIPA protein extract solution (cat. no. EBA-1147; Elpis Bio-tech, Inc.), in which Pierce™ Protease inhibitor mini tablets (cat. no. A32955) and Pierce™ Phosphatase inhibitor mini tablets (cat. no. A32957; both from Thermo Fisher Scientific, Inc.) were added. A total of 20 micrograms of total protein were quantitated using bicinchoninic acid (BCA) and loaded onto 5-20% E-pagel (cat. no. E-T520L; ATTO Corporation) filled with 1X Tris-Glycine SDS Buffer (cat. no. CBT015; LPS solution). The gels were transferred to a Q-blot kit (cat. no. WSE-4055; ATTO Corporation). After transfer, the PVDF membranes were blocked with 1X TBS buffer (cat. no. CBT005; LPS solution) containing 5% BSA (cat. no. BSAS0.1; Bovogen Biologicals) for 30 min at room temperature and incubated with indicated primary antibodies (1:1,000) overnight at 4˚C. Thereafter, the membranes were incubated with anti-mouse IgG (1:10,000) or anti-rabbit IgG horseradish peroxidase (HRP)-conjugated secondary antibodies (10,000) for 1 h at room temperature. Finally, the blots were developed by using an Immobilon® Western Chemiluminescent HRP substrate (cat. no. WBKLS0500; MilliporeSigma). Densitometric analysis was performed using Luminograph (cat. no. WSE-6100; software version ImageSaver 6; ATTO Corporation).

In vivo tumor xenograft model. Total 20 of Female CAnN. Cg-Foxn1nu/CrlOri (BALB/c nude) mice (8 weeks-old; weight, 21±1 g) were obtained from Orient Bio, Inc. The mice were acclimated for 1 week before experiment at a temperature of 24±1˚C with 45±5% humidity, and a 12/12-h light/dark cycle and were provided food and water *ad libitum*. The animals were injected subcutaneously with MDA-MB-231 cells ($5x10^6$ cells/mouse) in a mixture of phenol-red free RPMI and phenol-red free Matrigel (total volume of 100 μl at a 1:1 ratio). When the tumor size reached 50-60 mm^3, the animals were randomly classified into vehicle, CFI-402257, AICAR and combination groups (n=5 per group). CFI-402257 and the vehicle (10% NMP:40% PEG400:50% D.W.) were administered via oral gavage (P.O.), whereas AICAR (diluted in PBS) was administered via intraperitoneal (I.P.) injection (QD, 5 days/week). Tumor sizes and animal weight were measured. Animals was euthanized using a 50% per min displacement of chamber air with compressed CO_2. Tumor tissue sample was collected, images were captured and the weight was measured. Tumor volume was calculated using the standard formula: 0.52 x length x $width^2$. The tumor growth inhibition (TGI) rate was calculated using the following equation: $[1-(V_{f,\ drug\ treated}-V_{i,\ drug\ treated})/(V_{f,\ vehicle}-V_{i\ vehicle})]$ x100, where V_f was the average volume of tumor on the final day of the study, and V_i was the average volume of tumor on the first day of the study (24).

Statistical analysis. The experimental data were performed at least three times, and are expressed as the mean±SEM or the mean ± SD. For the determination of statistically significance, a one-way analysis of variance (ANOVA) was used and then compared it with Bonferroni's multiple comparison tests. $^*P<0.05$ was considered to indicate statistically significant differences between the control and the treatment groups. All of the statistical comparisons were performed using GraphPad Prism Software Version 8.0 (Dotmatics).

Results

Anticancer activity of CFI-402257, AICAR and their combination in MDA-MB-231 cells. Cytotoxicity of three Mps1/TTK inhibitors (CFI-402257, empesertib and BOS-172722) and three AMPK activators (AICAR, A-23187 and metformin) was tested either alone or in combination in MDA-MB-231 cells. AICAR and CFI-402257 were investigated alone or in combination to evaluate the enhanced anticancer effect of a combination of drugs. The viability of MDA-MB-231 cells treated with the combination of AICAR or metformin with CFI-402257 was reduced significantly compared with that of cells treated with all drugs alone (Figs. 1B, S1 and S2).

The inhibition of cell cytotoxicity after treatment with CFI-402257 and AICAR was examined in a normal breast cell line (HMEC) and a luminal BC cell line (MCF-7). As demonstrated in Fig. 1A, CFI-402257 selectively induced MDA-MB-231 TNBC cell cytotoxicity with high Mps1/TTK expression (Fig. 1C), whereas AICAR showed low selectivity in three breast cell lines. The combination therapy of CFI-402257 and AICAR was effective on both of MDA-MB-231 and MCF-7 cells. However, the combined effects were similar to that of AICAR alone in the MCF-7 cell line (Fig. 1B).

To validate the effects of CFI-402257 and AICAR on their respective targets, the expression levels of p-TTK, TTK, p-AMPK and AMPK were determined using western blot analysis. The robust SAC was activated by a spindle poison, nocodazole (50 ng/ml), to determine SAC modulation by Mps1/TTK inhibitors (25). Mps1/TTK dephosphorylation by Mps1/TTK inhibitors was evaluated (15,24). Combination therapy with CFI-402257 and AICAR showed synergistic

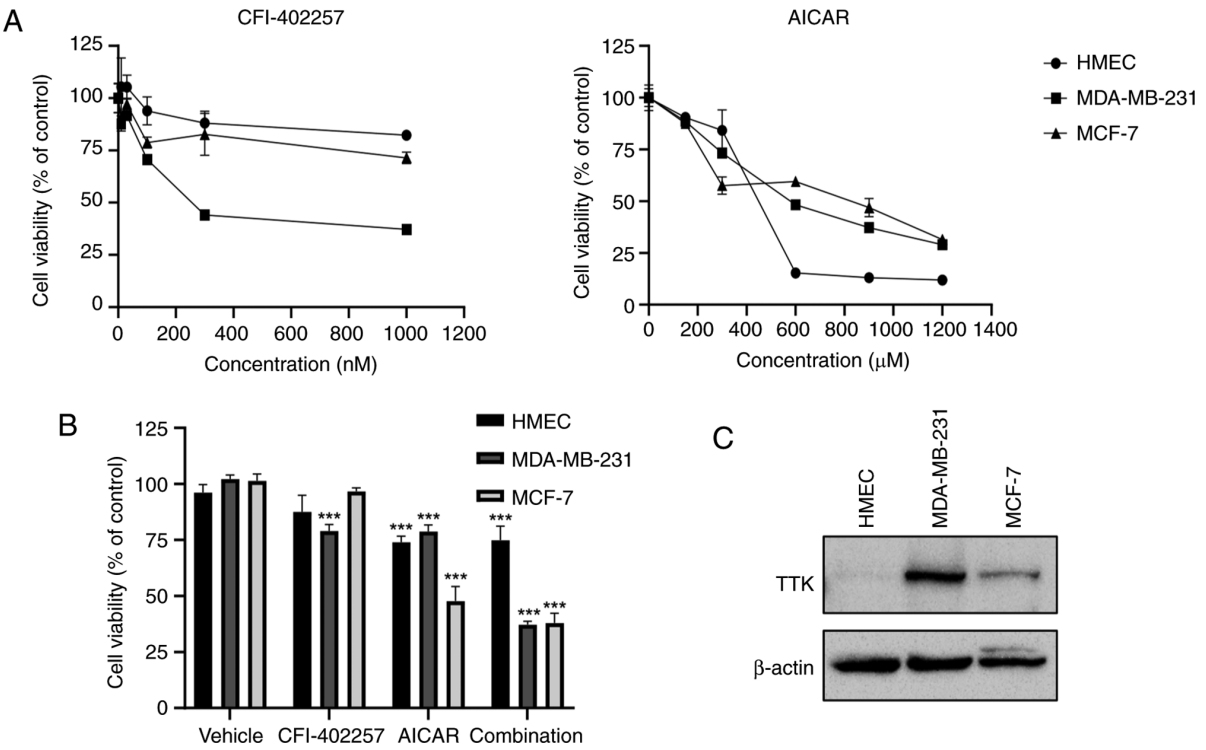

Figure 1. Selective cytotoxicity on a combination of CFI-402257 and AICAR in MDA-MB-231 cells. (A) Cytotoxicity of CFI-402257 and AICAR against three breast cell lines. Cells were treated with various concentrations of CFI-402257 (0, 30, 100, 300 and 1,000 nM) and AICAR (150, 300, 600, 900 and 1,200 μM) for 72 h. (B) Cytotoxicity of monotherapy and combination therapy (CFI-402257: 100 nM, AICAR: 300 μM) in the three breast cell lines for 72 h. The values represent the mean ± SEM. ***P<0.001 vs. the control group. (C) Basal TTK expression levels in the three breast cell lines were determined by western blot analysis.

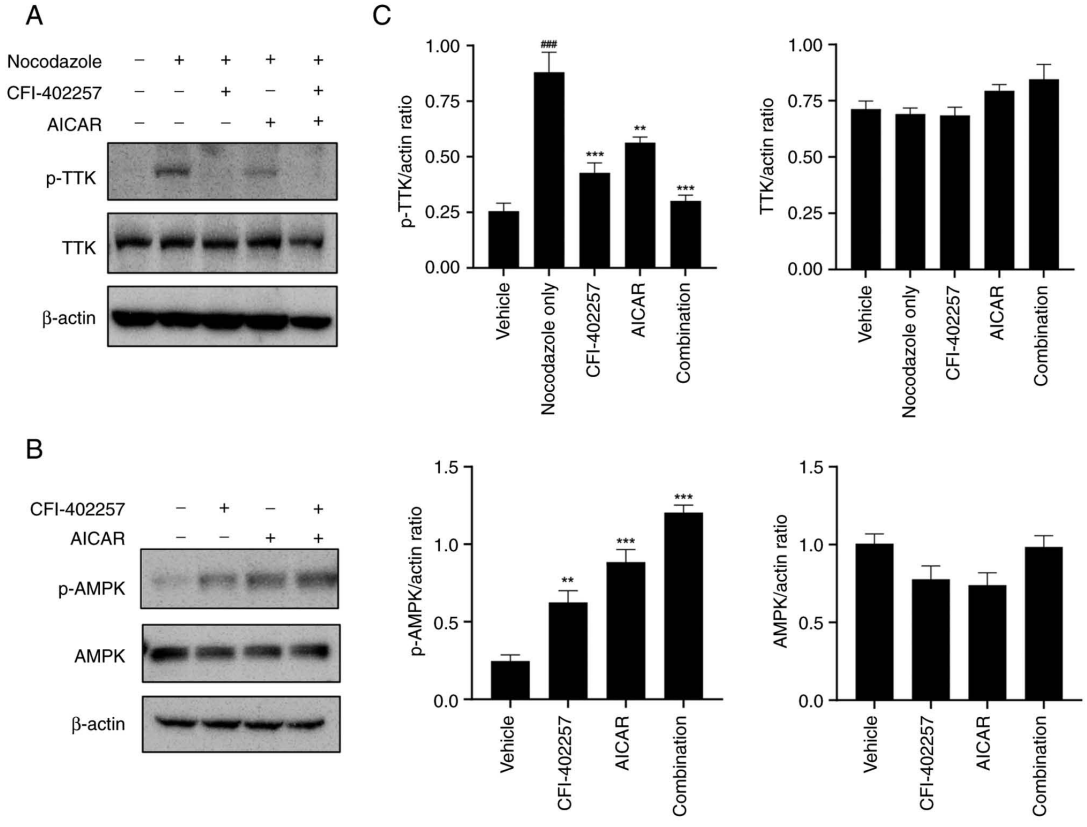

Figure 2. Effects of CFI-402257 and AICAR on the main target proteins in MDA-MB-231 cells. (A) Western blot analysis of p-TTK and TTK. Cells were pretreated with 50 ng/ml nocodazole for 17 h before treatment with CFI-402257 and AICAR and their combination for 4 h. (B) Western blot analysis of p-AMPK and AMPK. Cells were treated with CFI-402257 and AICAR and their combination for 24 h. (C) Representative histogram of protein expression levels. The values represent the mean ± SEM. $^{###}$P<0.001 vs. nocodazole group; **P<0.01 and ***P<0.001 vs. the control group. p-, phosphorylated.

A

	G0/G1	S	G2/M	Polyploid (>4n)
Vehicle	49.9±0.9	16.3±0.3	24.4±0.5	9.4±0.6
CFI-402257	35.4±0.1	16.2±0.4	30.7±0.2	17.7±0.2**
AICAR	51.6±0.8	20.6±0.1	20.3±1.0	7.5±0.6
Combination	40.5±0.7	19.4±0.2	27.3±0.1	12.8±0.6##

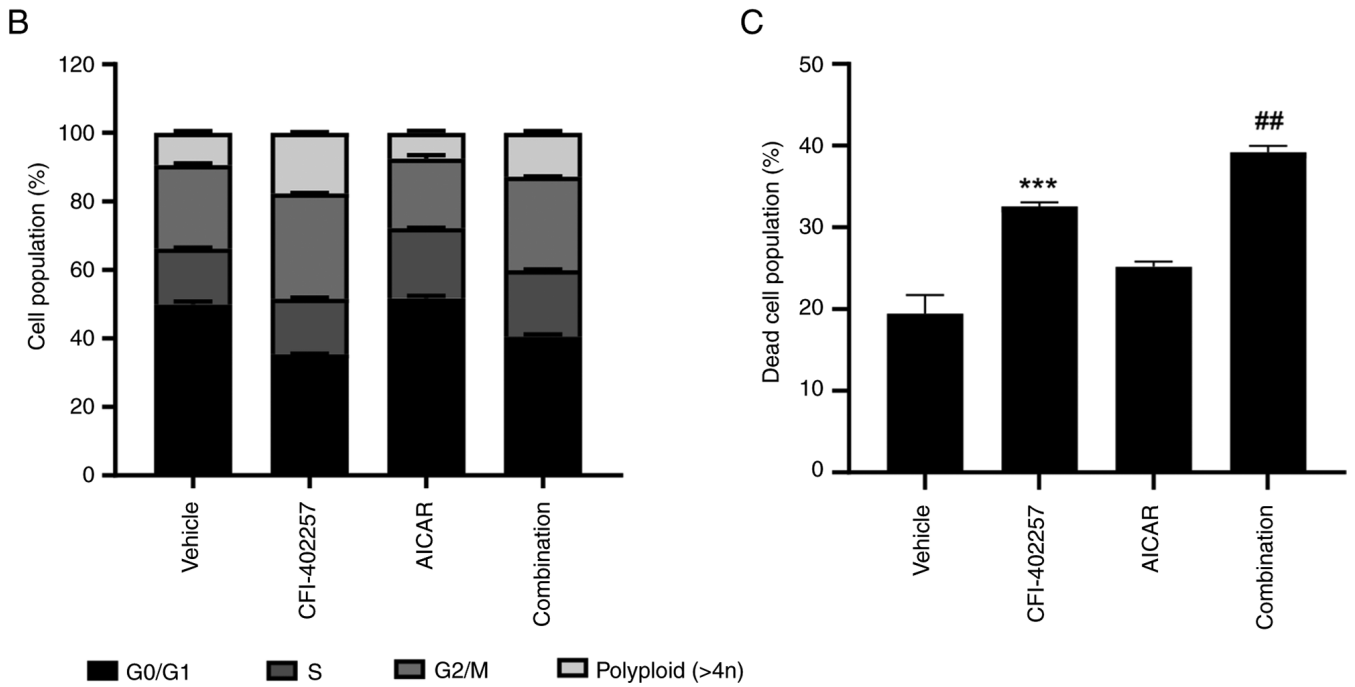

Figure 3. Cell-cycle distribution of MDA-MB-231 cells after treatment with the combination of CFI-402257 and AICAR. Cells were treated with CFI-402257 and AICAR for 72 h and stained with propidium iodide and analyzed by Muse™ Cell Analyzer. (A and B) The bar diagrams show the number of cells in the G0/G1, S, G2/M and polyploidy phases in the MDA-MB-231 cell line. Polyploidy was defined by the presence of more than 4n chromosomes. (C) The proportion of dead cells (%) in the ungated part of the samples. Data are shown as the mean ± SEM (n=3). **P<0.01 and ***P<0.001 vs. the control group; ##P<0.01 vs. the CFI-402257 treatment group.

effects by decreasing p-TTK and increasing p-AMPK protein levels (Figs. 2 and S3).

Cell-cycle distribution after combination therapy with CFI-402257 and AICAR. CFI-402257 increased the proportion of G2/M phase (24.4-30.7%) and polyploid cells (9.4-17.7%), while AICAR slightly increased the proportion of cells in the S phase (16.3-20.6%). Interestingly, the combination therapy group revealed decreased proportions of G2/M phase and polyploid cells and induced a higher cell death rate than the CFI-402257 monotherapy group (Fig. 3). The regulatory proteins involved in cell-cycle distribution were also evaluated using western blot analysis. Combination therapy reduced the levels of cyclin D1, cyclin E, p-cdc2 and cyclin-dependent kinase 2 (cdk2) in MDA-MB-231 cells. The protein level of cyclin B1 decreased slightly. Lastly, combination therapy significantly increased the protein levels of p27 (Figs. 4 and S3).

Apoptosis induced by combination therapy with CFI-402257 and AICAR. Annexin V-7AAD double-staining was performed to evaluate cell death induced by the combination of CFI-402257 and AICAR. Live (annexin V^-, 7-AAD^-), early apoptotic (annexin V^+, 7-AAD^+), late apoptotic (annexin V^+, 7-AAD^+), and dead (annexin V^-, 7-AAD^+) cells were identified using a Muse® Cell Analyzer. The total number of apoptotic cells was calculated by adding the early and late apoptotic cells. As demonstrated in Figs. 5A, B and S4, the combination therapy significantly increased the rate of total apoptosis in MDA-MB-231 cells in comparison with the CFI-402257 monotherapy group (28.5 vs. 47.3%). In addition, the expression levels of apoptosis-related proteins were analyzed using western blotting. Combination therapy increased the levels of cleaved poly (ADP-ribose) polymerase, cleaved caspase-3 and Bax in MDA-MB-231 cells. The cytoplasmic release of cytochrome C also increased, and the Bcl2 level was decreased. Overall, the Bax/Bcl2 ratio, a marker of apoptosis,

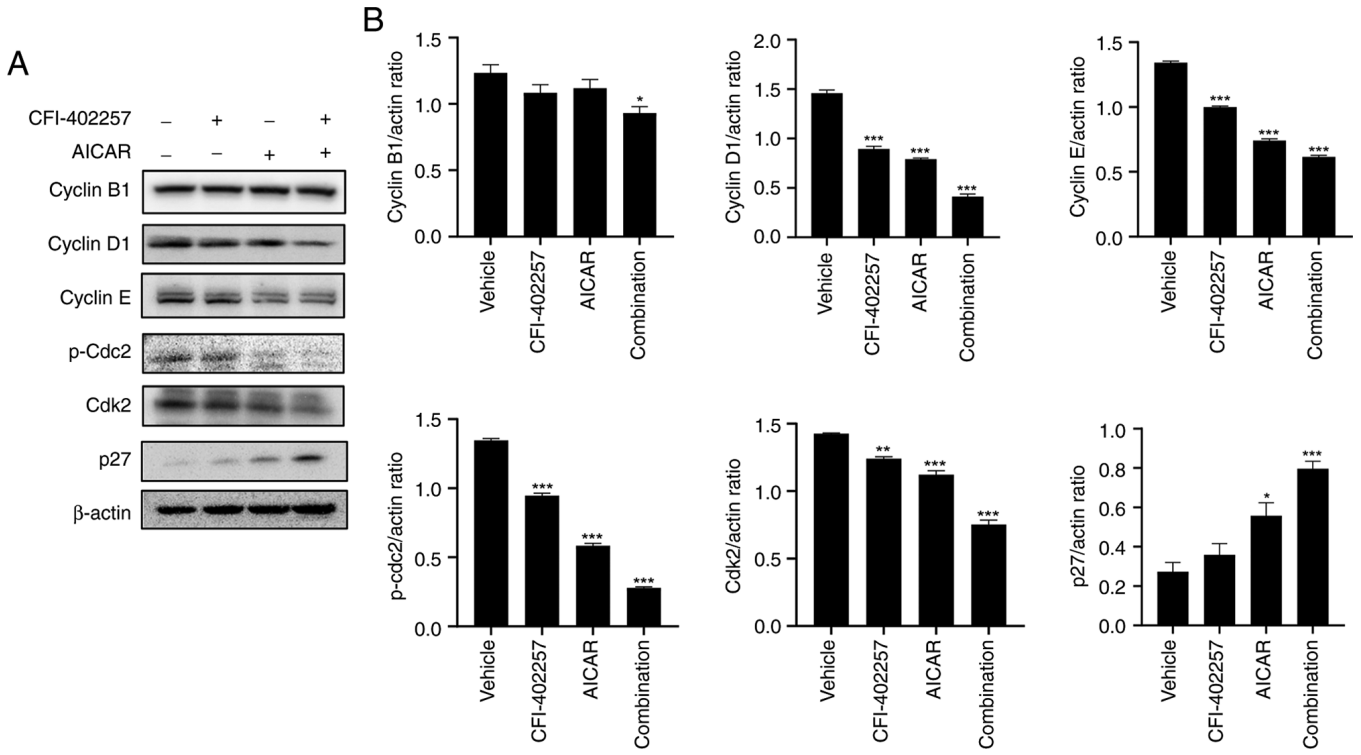

Figure 4. Effects of the combination of CFI-402257 and AICAR on cell cycle related proteins in MDA-MB-231 cells. (A) Western blot analysis of cyclin protein, CDK-related protein and p27. (B) Representative histogram of protein expression level. Data are shown as the mean ± SEM (n=3). *P<0.05, **P<0.01 and ***P<0.001 vs. the control group.

increased (Figs. 5C and D and S3). These results indicated that combination therapy with CFI-402257 and AICAR effectively induced apoptosis.

Autophagic cell death after combination therapy with CFI-402257 and AICAR. To improve understanding of the mechanisms underlying cell death, AO staining (which changes to bright red under acidic conditions) was used to highlight autophagosomes (26). The combination therapy with CFI-402257 and AICAR significantly increased the number of acidic vacuoles. Both monotherapies also induced the formation of acidic vacuoles (Fig. 6A). Another marker of autophagosomes, LC3B-II (membrane-bound form, lower band), was also significantly upregulated in the combination group. The expression levels of other autophagy-related proteins, namely, Beclin-1, Atg3 and Atg7, also increased in the combination therapy group (Figs. 6B, C and S3). Thus, combination therapy with CFI-402257 and AICAR mediated autophagic cell death in MDA-MB-231 cells. Western blot analysis was used to determine the effect of combination therapy on the PI3K/Akt/mTOR and MAPK pathways; it was revealed that the expression levels of p-PI3K, p-Akt, p-mTOR and Akt were downregulated, while the expression of the tumor suppressor regulator PTEN, which inhibits the Akt/mTOR signaling pathway (27), increased in the combination therapy group (Figs. 7 and S3). The expression levels of p-ERK, p-JNK and p-p38 were also downregulated in the combination therapy group (Figs. 8 and S3).

The combination of CFI-402257 and AICAR effectively inhibits TNBC growth in the tumor xenograft model. The *in vivo* antitumor activity of the compounds was examined in mice bearing MDA-MB-231 tumor xenografts. After the treatment, the longest tumor lengths observed were 14.33, 7.36, 7.92 and 5.85 mm in the vehicle group, CFI-402257 monotherapy, AICAR monotherapy and the combination therapy group, respectively. Correspondingly, the final mean tumor volumes were calculated as 297.9 mm^3 (range, 133.4~485.28 mm^3), 132.04 (range, 64~179.06 mm^3), 123.12 (range, 83.7~153.32 mm^3) and 60.96 mm^3 (range, 30.61~101.63 mm^3) for the vehicle treatment, CFI-402257 alone, AICAR alone, and the combination treatment, respectively. Complete inhibition of tumor growth was observed in the combination group, with a TGI rate of 98%, whereas the TGI rates for monotherapy with CFI-402257 and AICAR were 69 and 71%, respectively (Fig. 9). No significant adverse effects, such as weight loss (>10% of total weight) or strange behaviors, were observed in the studies.

Discussion

Mps1/TTK, which is the core protein of the SAC complex, is overexpressed in TNBC in comparison with other BC cells (9-12). Mps1/TTK inhibition triggers genomic instability and results in cancer cell apoptosis. Aneuploid cancer cells show resistance to multiple chemotherapeutic regimens, induce tumor heterogeneity, and improve the tumors' adaptation to harsh conditions (28,29). In particular, highly aneuploid cancer cells are more sensitive to the energy and proteotoxic stress induced by AMPK agonists than normal cells (20,30,31). Therefore, the synergistic effect of the MPS1/TTK inhibitor (which increases aneuploidy) with proteotoxic compounds that

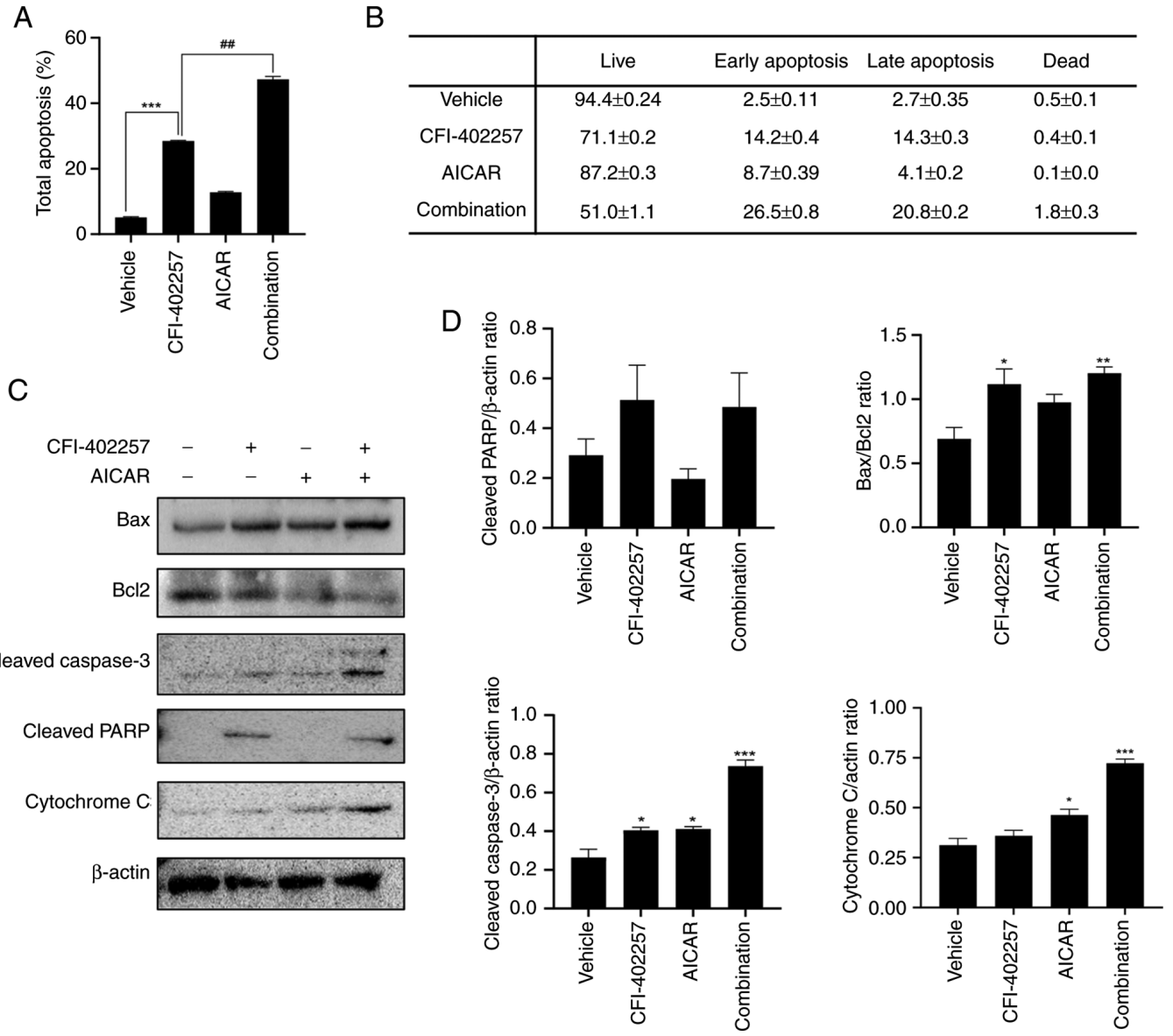

	Live	Early apoptosis	Late apoptosis	Dead
Vehicle	94.4±0.24	2.5±0.11	2.7±0.35	0.5±0.1
CFI-402257	71.1±0.2	14.2±0.4	14.3±0.3	0.4±0.1
AICAR	87.2±0.3	8.7±0.39	4.1±0.2	0.1±0.0
Combination	51.0±1.1	26.5±0.8	20.8±0.2	1.8±0.3

Figure 5. Effects of the combination of CFI-402257 and AICAR on apoptotic cell death in MDA-MB-231 cells. The cells were treated with CFI-402257 and AICAR for 72 h and evaluated by the annexin V-7AAD double-staining method. (A) Histogram showing the percentage of total apoptosis. (B) Table showing the percentage of live cells, early apoptosis, late apoptosis and dead cells. (C) Expression levels of apoptosis-related proteins were analyzed by western blotting. (D) Representative histogram of protein expression levels. The values represent the mean ± SEM. *P<0.05, **P<0.01 and ***P<0.001 vs. the control group; $^{\#\#}$P<0.01 vs. the CFI-402257 treatment group. PARP, poly (ADP-ribose) polymerase.

perturb energy metabolism was investigated in the present study.

To evaluate the anticancer effects of the MPS1/TTK inhibitor in combination with a proteotoxic compound, cancer cell cytotoxicity was evaluated after exposure to combinations of three Mps1/TTK inhibitors (CFI-402257, Empesertib and BOS-172722) and three AMPK activators (AICAR, A-23187 and Metformin). As demonstrated in Fig. S2, the three Mps1/TTK inhibitors showed similar cytotoxic potency with each AMPK activator. However, A-23187 exhibited less synergism than the other AMPK activators. Metformin is an indirect AMPK activator that inhibits complex 1 in the mitochondrial respiratory chain and eventually increases the AMP:ATP ratio by inhibiting oxidative phosphorylation (OXPHOS). However, numerous resistant cancer cells produce ATP via glycolysis rather than OXPHOS even in the presence of oxygen, a phenomenon called the Warburg effect. Thus, inhibition of OXPHOS may cause activation of glycolysis, which could result in resistance. By contrast, AICAR is an allosteric AMPK activator that mimics the structure of AMP, potentially allowing it to act on AMPK while causing fewer changes in OXPHOS and glycolysis than metformin (19,32,33). Previous studies have also reported that AICAR is effective against aneuploid cancer cells, but metformin is not (20,34). Therefore, the subsequent studies were conducted using CFI-402257, an MPS1/TTK inhibitor, and AICAR, an AMPK activator.

The *in vitro* anticancer effects of CFI-402257, AICAR and their combination were tested in three breast cell lines: HMECs, MCF-7 and MDA-MB-231. The MDA-MB-231 cell line is commonly used as late-stage BC model. This cell line is ER^{-}, PR^{-} and HER2-negative and expresses mutated p53. Therefore, MDA-MB-231 represents a favorable model

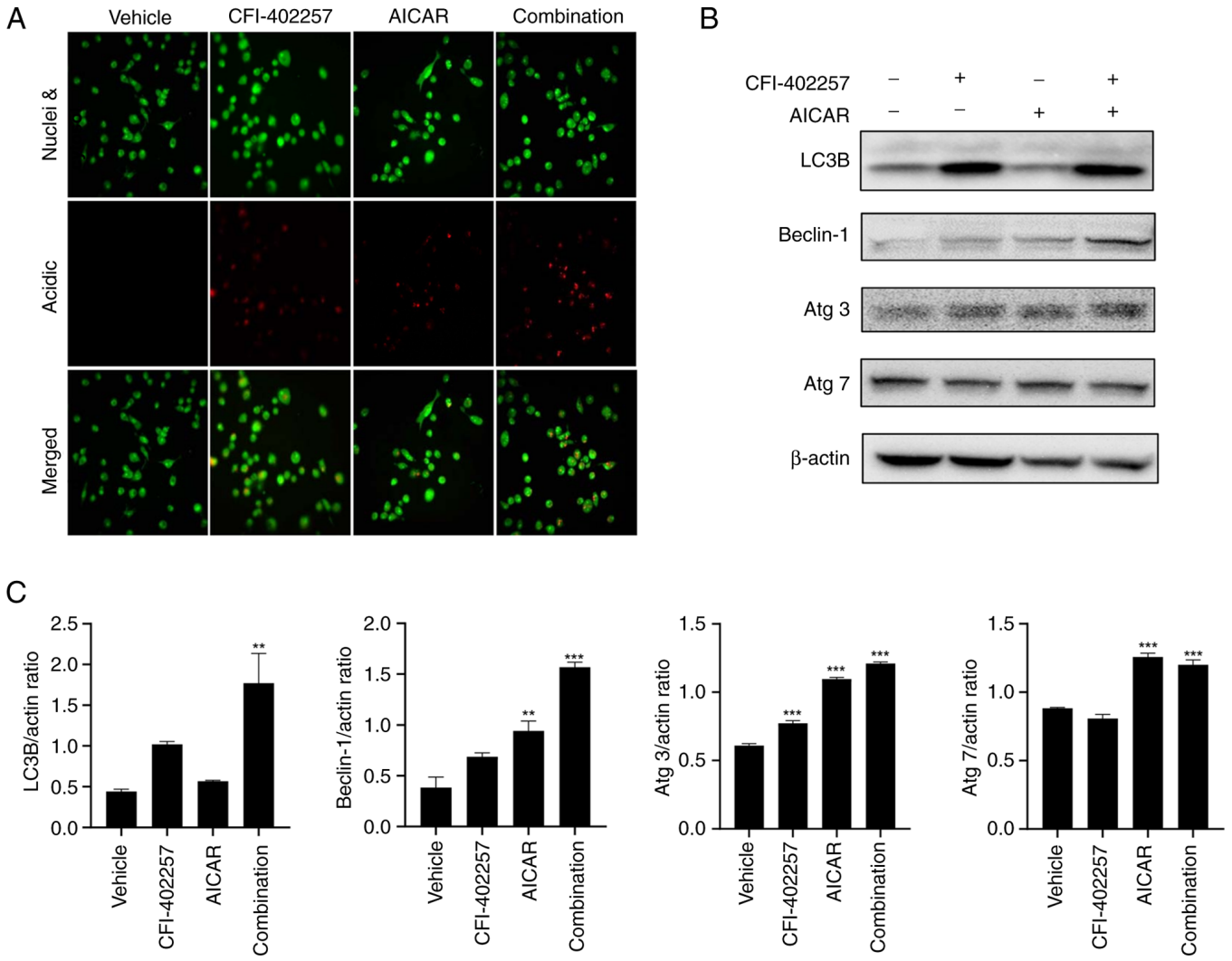

Figure 6. Autophagic cell death in MDA-MB-231 cells by the combination of CFI-402257 and AICAR. (A) Cells were stained with acridine orange after treatment with CFI-402257 and AICAR for 72 h. Images observed under a confocal laser scanning microscope (K1-Fluo; magnification, x200) (B) Expression levels of autophagy-related proteins analyzed by western blots. (C) Representative histogram of protein expression levels. The values represent the mean ± SEM. **P<0.01 and ***P<0.001 vs. the control group.

of TNBC. CFI-402257 exhibited the most potent effect on MDA-MB-231 cells. HMECs may be more vulnerable to the energy stress induced by AICAR than cancer cells. AICAR monotherapy exhibited cytotoxicity in the MCF-7 cell line. The cytotoxicity of the drug combination was compared with that of each drug treated alone to evaluate the beneficial effects of combination therapy. The combination of AICAR with CFI-402257 resulted in a notable decrease in the viability of MDA-MB-231 cells compared with when each drug treated alone. In MCF-7 cells, the combination of CFI-402257 and AICAR exhibited cytotoxicity, while the combined effects were similar to that of AICAR alone. Based on the results of combination therapy, expanding the indication to include ER$^+$ BC patients with high Mps1/TTK expression could be considered. Phosphorylation of Mps1/TTK is activated only in the tumor microenvironment; nocodazole, which interferes with microtubule polymerization, was treated with other test compounds to evaluate changes in p-Mps1/TTK level (7,24,35). In the present study, CFI-402257 and AICAR synergistically inhibited cell proliferation and decreased p-Mps1/TTK and p-AMPK protein levels in MDA-MB-231 cells.

The SAC inhibition and massive chromosome segregation caused by CFI-402257 affect cell-cycle distribution (24). In the CFI-402257 treatment group, the levels of G2/M phase and polyploid cell counts were substantially greater than those in the vehicle group. By contrast, in the AICAR treatment group, the cell counts in the G0/G1 and S phases were slightly greater than those in the vehicle group. Notably, the annexin V apoptosis assay showed that the apoptotic rate increased significantly with combined treatment with CFI-402257 and AICAR. The potential benefits of utilizing an AMPK agonist against various high-grade aneuploid human tumors was proposed (20). In the present study, the heightened apoptosis induced by AICAR was observed in states of increased aneuploidy, facilitated by the Mps1/TTK inhibitor (36). Future studies to investigate the anticancer effects on sorted polyploidy cells are required to understand the aneuploidy sensitivity of AMPK agonist.

Apoptosis via the intrinsic pathway by Mps1/TTK inhibitors has been widely reported, whereas autophagic

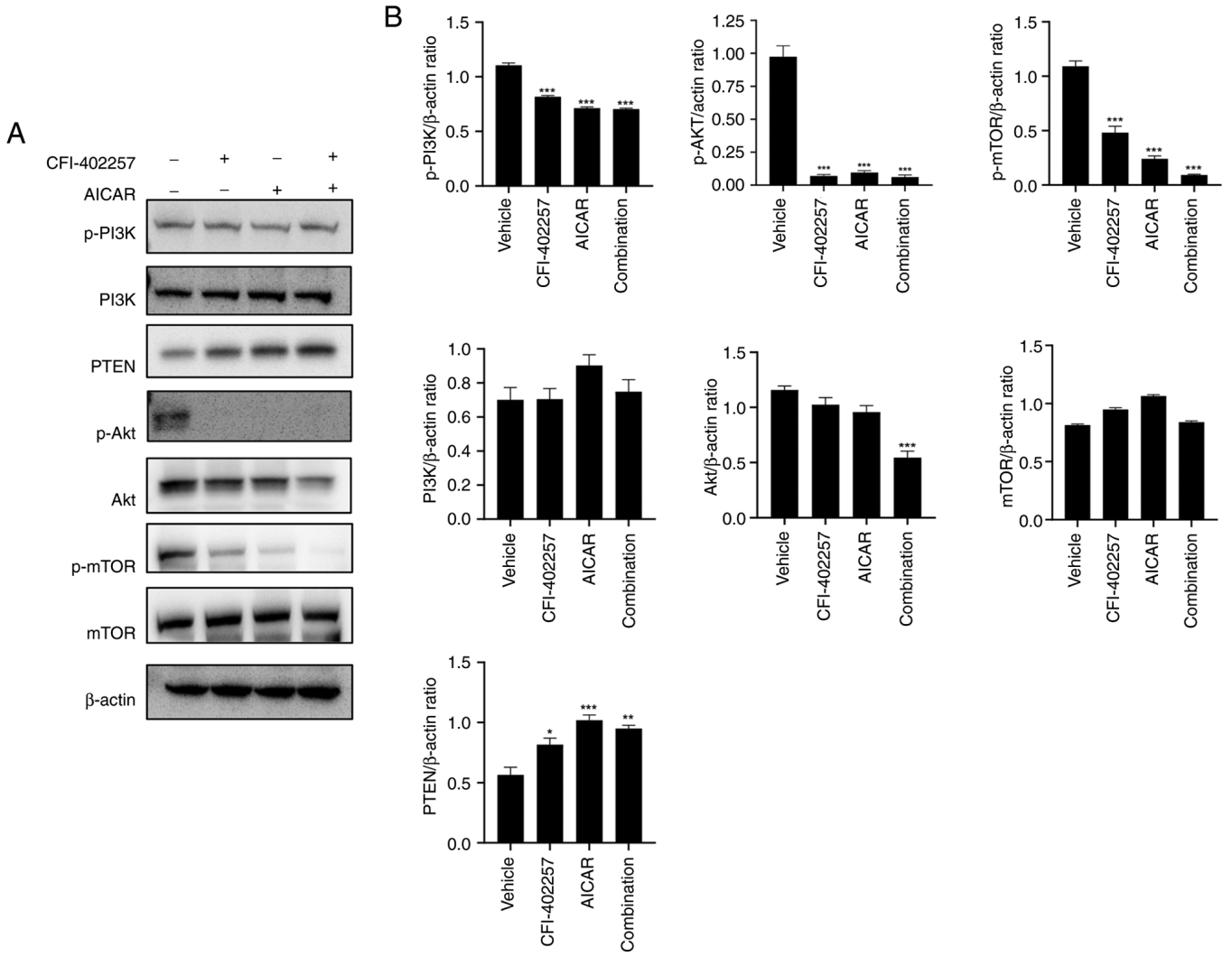

Figure 7. Inhibition of the PI3K/Akt/mTOR signaling pathway by the combination of CFI-402257 and AICAR. (A) Western blot analysis of the expression levels of PI3K/Akt/mTOR-related proteins in MDA-MB-231 cells. (B) Representative histogram of the protein expression levels. The values represent the mean ± SEM. *P<0.05, **P<0.01 and ***P<0.001 vs. the control group. p-, phosphorylated.

cell death has rarely been studied. To understand the precise molecular mechanisms underlying this form of cell death, changes in autophagy biomarkers were investigated, and the combination of CFI-402257 and AICAR revealed dual inhibition of the PI3K/Akt/mTOR and MAPK pathways (Figs. 7 and 8). The PI3K/Akt/mTOR-PTEN axis is considered the predominant oncogenic pathway that is mutated in BC. In particular, frequent alterations have been observed in PTEN, which plays a crucial role in TNBC. Therefore, numerous clinical attempts using PI3K/mTOR inhibitors have been made for TNBC treatment. The MAPK signaling pathway consists of three main groups: Extracellular signal-regulated protein kinases (ERK1/2), p38 MAP kinases and c-Jun NH2-terminal kinases (JNK1/2/3), which are associated with various malignancies, including breast, lung and thyroid carcinomas as well as neck squamous cell carcinomas. The MAPK pathway is frequently hyperactive in TNBC. One reason for this is that TNBC shows aggressive division along with an increased number of genomic copies in comparison with other BC cells. This leads to genomic instability in these cells. Second, the loss of crosstalk between other signaling pathways, such as the PI3K/Akt/mTOR pathway, may cause uncontrolled MAPK pathway activation. Therefore, dual targeting of the PI3K/Akt/mTOR and MAPK pathways is important to effectively inhibit the cytotoxicity of TNBC (37-39). Thus, the dual inhibition of the PI3K/Akt/mTOR and MAPK pathways induced by the combination of CFI-402257 and AICAR could be a potential strategy for treating TNBC.

Interestingly, protein expression level of p27 was increased (Fig. 4). The critical role of p27 in regulating G1-to-S phase progression and its prognostic significance have been reported in several BC studies (40). p27 is eliminated by ubiquitin-mediated proteolysis, and its degradation is inhibited by decreased cyclin expression. Several investigators have reported the effect of PI3K/Akt and Ras/Raf/Mek1 pathways on the abundance and activity of p27. Considering the present study, the PI3K/Akt pathway was inhibited by combination therapy. Inhibition PI3K/Akt pathway suppresses the expression of oncogenes such as c-myc. Therefore, the expression of p27, which are regulated by c-myc, was increased (41).

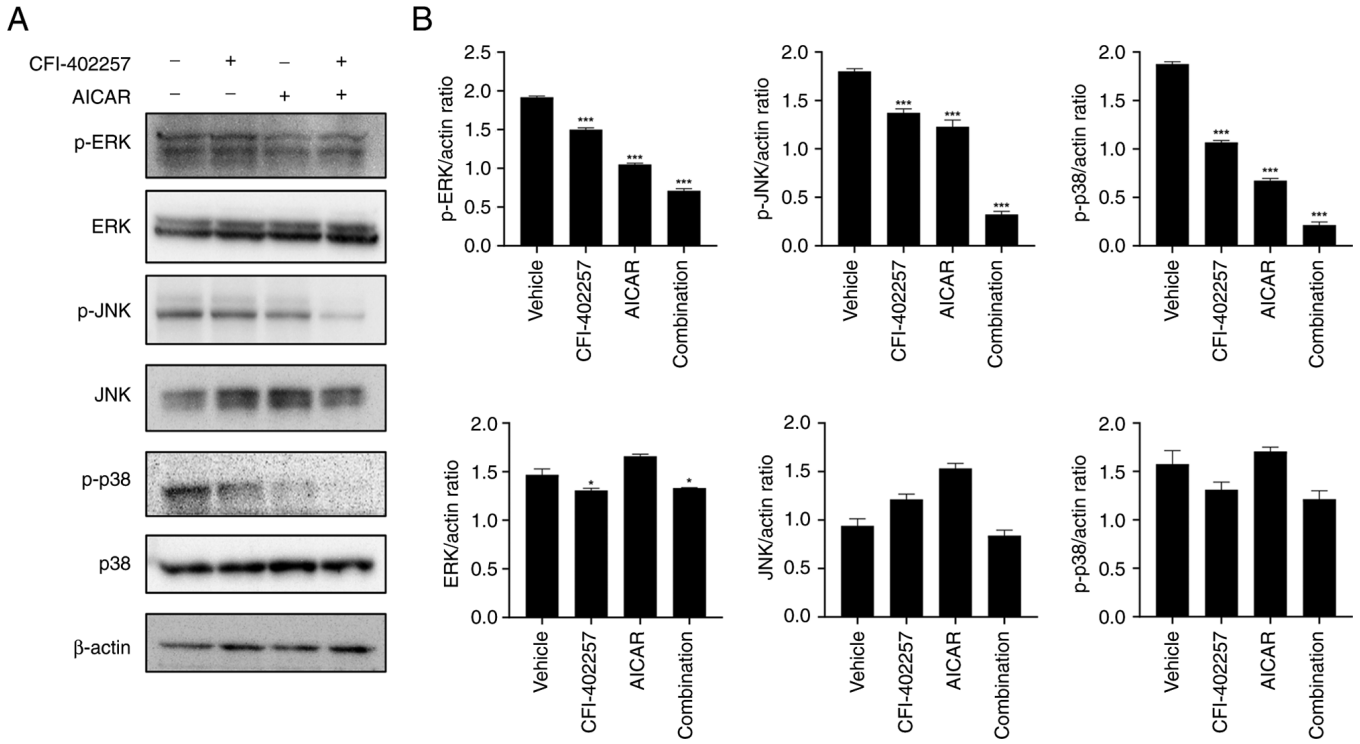

Figure 8. Inhibition of the MAPK signaling pathway by combined treatment with CFI-402257 and AICAR. (A) Western blot analysis of the expression levels of MAPK-related proteins in MDA-MB-231 cells. (B) Representative histogram of the protein expression level. The values represent the mean ± SEM. *P<0.05 and ***P<0.001 vs. the control group. p-, phosphorylated.

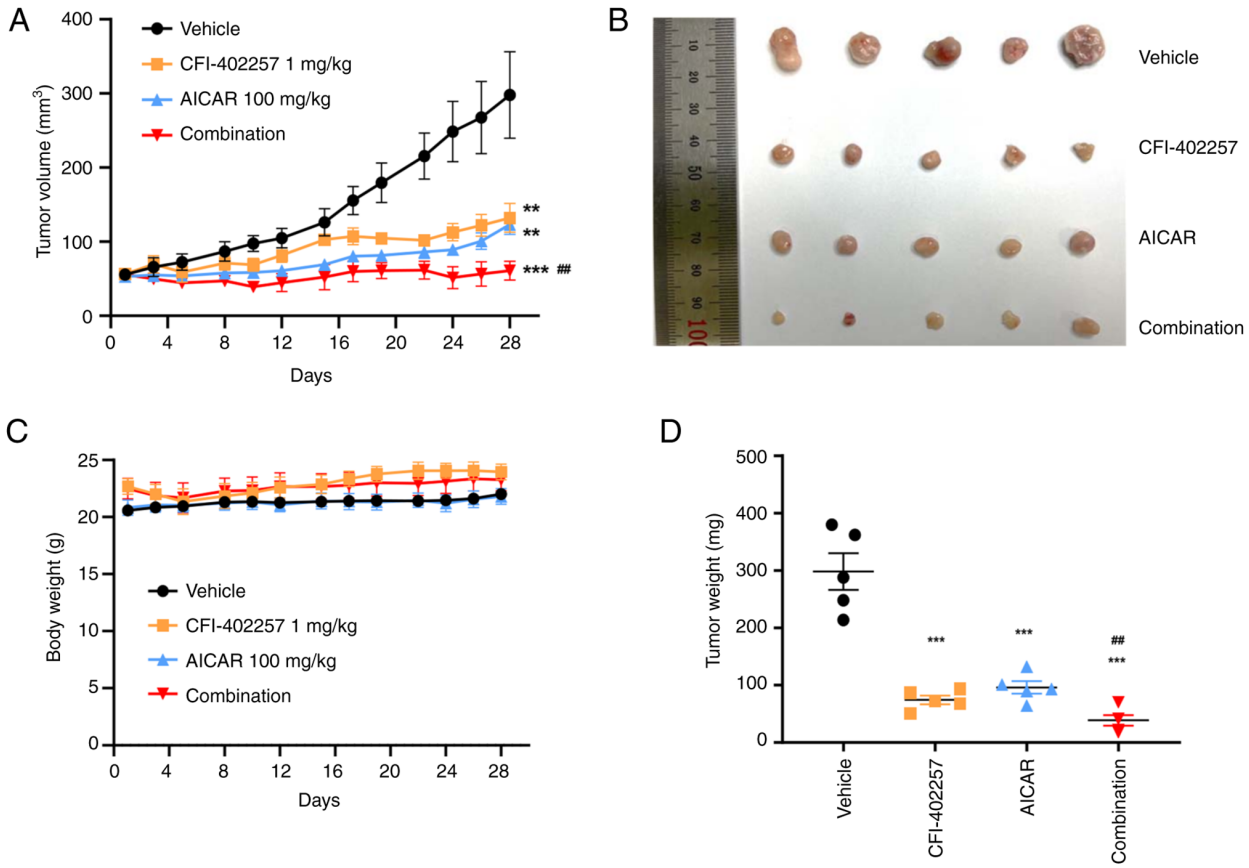

Figure 9. Anticancer effect of the combination of CFI-402257 with AICAR on an *in vivo* tumor MDA-MB-231 xenograft model. (A) Athymic nude mice bearing MDA-MB-231 xenografts were administered CFI-402257 (1 mg/kg, QD, P.O.), AICAR (100 mg/kg, QD, I.P.) and their combination for 28 days. Tumor volume was measured once every 2 days. (B) Representative image of the tumor. (C) Body weight changes in nude mice. (D) Tumor weight changes in each group. The values represent the mean ± SD (n=5). **P<0.01 and ***P<0.001 vs. the control group; $^{\#\#}$P<0.01 vs. the CFI-402257 treatment group.

The main limitation of the application of Mps1/TTK inhibitors *in vivo* is their narrow therapeutic range due to hematological and gastrointestinal toxicities. The maximum tolerable dose of CFI-402257 in mice is 6.5 mg/kg (24). Considering the *in vivo* profile results and the study designs of previous investigations on CFI-402257 and AICAR (24,42,43), the dosages for the combination therapy were chosen as 1 mg/kg for CFI-402257 and 100 mg/kg for AICAR in the present study. This combination inhibited tumor growth by 98% without any additional adverse effects; in comparison, the inhibition rates with CFI-402257 and AICAR monotherapy were 69 and 71%, respectively (Fig. 9). The expression of markers related to mechanisms such as the cell cycle, cell viability and apoptosis in tumor tissues was not measured and it will be considered in the further study. To the best of the author's knowledge, the present study provides the first *in vivo* evidence for the anticancer activity study of a combination of an Mps1/TTK inhibitor and an AMPK activator.

In conclusion, to circumvent the excessive toxicity of Mps1/TTK inhibitors, a combination of an Mps1/TTK inhibitor with an AMPK agonist was explored in the present study. The combination therapy showed enhanced anticancer effect mediated by dual inhibition of the PI3K/Akt/mTOR and MAPK pathways, which regulate cell cytotoxicity, apoptosis and autophagy. The combination of CFI-402257 and AICAR significantly suppressed the growth of MDA-MB-231-derived TNBC in immunodeficient mice. These findings provide new insights into the potential for using CFI-402257 in combination with an AMPK agonist to enhance its efficacy and tolerability in TNBC therapy.

Acknowledgements

Not applicable.

Funding

The present study was supported by the Korea Drug Development Fund funded by the Ministry of Science and ICT, Ministry of Trade, Industry, and Energy, and Ministry of Health and Welfare (grant no. HN22C0694; Republic of Korea).

Availability of data and materials

The data generated in the present study may be requested from the corresponding author.

Authors' contributions

JSL, JS and SA designed the experiments. JSL performed the experiments. SA, JSL and EK analyzed and interpreted the data. SA, JSL, and EK wrote and revised the manuscript. JS and SA supervised the study and confirm the authenticity of all the raw data. All authors read and approved the final manuscript.

Ethics approval and consent to participate

All applicable national and institutional guidelines for the care and use of animals were followed. The protocols for animal experiments were approved (approval no. 2021-7F-08-02; approval date: 2022-08-27) by the Animal Ethics Committee of the Korea Research Institute of Chemical Technology with code number (Daejeon, Korea). The study was carried out in compliance with the ARRIVE guidelines.

Patient consent for publication

Not applicable.

Competing interests

The authors declare that they have no competing interests.

References

1. Siegel RL, Miller KD and Jemal A: Cancer statistics, 2018. CA Cancer J Clin 68: 7-30, 2018.
2. Sasmita AO and Wong YP: Organoids as reliable breast cancer study models: An update. Int J Oncol Res 1: 008, 2018.
3. Schwentner L, Wolters R, Koretz K, Wischnewsky MB, Kreienberg R, Rottscholl R and Wöckel A: Triple-negative breast cancer: The impact of guideline-adherent adjuvant treatment on survival-a retrospective multi-centre cohort study. Breast Cancer Res Treat 132: 1073-1080, 2012.
4. Bai L, Zhou B, Yang CY, Ji J, McEachern D, Przybranowski S, Jiang H, Hu J, Xu F, Zhao Y, *et al*: Targeted degradation of BET proteins in triple-negative breast cancer. Cancer Res 77: 2476-2487, 2017.
5. Dominguez-Brauer C, Thu KL, Mason JM, Blaser H, Bray MR and Mak TW: Targeting mitosis in cancer: Emerging strategies. Mol Cell 60: 524-536, 2015.
6. Lara-Gonzalez P, Westhorpe FG and Taylor SS: The spindle assembly checkpoint. Curr Biol 22: R966-R980, 2012.
7. Colombo R, Caldarelli M, Mennecozzi M, Giorgini ML, Sola F, Cappella P, Perrera C, Depaolini SR, Rusconi L, Cucchi U, *et al*: Targeting the mitotic checkpoint for cancer therapy with NMS-P715, an inhibitor of MPS1 kinase. Cancer Res 70: 10255-10264, 2010.
8. Tardif KD, Rogers A, Cassiano J, Roth BL, Cimbora DM, McKinnon R, Peterson A, Douce TB, Robinson R, Dorweiler I, *et al*: Characterization of the cellular and antitumor effects of MPI-0479605, a small-molecule inhibitor of the mitotic kinase Mps1. Mol Cancer Ther 10: 2267-2275, 2011.
9. Maire V, Baldeyron C, Richardson M, Tesson B, Vincent-Salomon A, Gravier E, Marty-Prouvost B, De Koning L, Rigaill G, Dumont A, *et al*: TTK/hMPS1 is an attractive therapeutic target for triple-negative breast cancer. PLoS One 8: e63712, 2013.
10. Salvatore G, Nappi TC, Salerno P, Jiang Y, Garbi C, Ugolini C, Miccoli P, Basolo F, Castellone MD, Cirafici AM, *et al*: A cell proliferation and chromosomal instability signature in anaplastic thyroid carcinoma. Cancer Res 67: 10148-10158, 2007.
11. Slee RB, Grimes BR, Bansal R, Gore J, Blackburn C, Brown L, Gasaway R, Jeong J, Victorino J, March KL, *et al*: Selective inhibition of pancreatic ductal adenocarcinoma cell growth by the mitotic MPS1 kinase inhibitor NMS-P715. Mol Cancer Ther 13: 307-315, 2014.
12. Yuan B, Xu Y, Woo JH, Wang Y, Bae YK, Yoon DS, Wersto RP, Tully E, Wilsbach K and Gabrielson E: Increased expression of mitotic checkpoint genes in breast cancer cells with chromosomal instability. Clin Cancer Res 12: 405-410, 2006.
13. Fuentes-Antrás J, Bedard PL and Cescon DW: Seize the engine: Emerging cell cycle targets in breast cancer. Clin Transl Med 14: e1544, 2024.
14. Martinez R, Blasina A, Hallin JF, Hu W, Rymer I, Fan J, Hoffman RL, Murphy S, Marx M, Yanochko G, *et al*: Mitotic checkpoint kinase Mps1 has a role in normal physiology which impacts clinical utility. PLoS One 10: e0138616, 2015.
15. Anderhub SJ, Mak GW, Gurden MD, Faisal A, Drosopoulos K, Walsh K, Woodward HL, Innocenti P, Westwood IM, Naud S, *et al*: High proliferation rate and a compromised spindle assembly checkpoint confers sensitivity to the MPS1 inhibitor BOS172722 in triple-negative breast cancers. Mol Cancer Ther 18: 1696-1707, 2019.

16. Wengner AM, Siemeister G, Koppitz M, Schulze V, Kosemund D, Klar U, Stoeckigt D, Neuhaus R, Lienau P, Bader B, *et al*: Novel Mps1 kinase inhibitors with potent antitumor activity. Mol Cancer Ther 15: 583-592, 2016.
17. Novais P, Silva PMA, Amorim I and Bousbaa H: Second-generation antimitotics in cancer clinical trials. Pharmaceutics 13: 1011, 2021.
18. Atrafi F, Boix O, Subbiah V, Diamond JR, Chawla SP, Tolcher AW, LoRusso PM, Eder JP, Gutierrez M, Sankhala K, *et al*: A phase I study of an MPS1 inhibitor (BAY 1217389) in combination with paclitaxel using a novel randomized continual reassessment method for dose escalation. Clin Cancer Res 27: 6366-6375, 2021.
19. Kim J, Yang G, Kim Y, Kim J and Ha J: AMPK activators: Mechanisms of action and physiological activities. Exp Mol Med 48: e224, 2016.
20. Tang YC, Williams BR, Siegel JJ and Amon A: Identification of aneuploidy-selective antiproliferation compounds. Cell 144: 499-512, 2011.
21. Vasudevan A, Schukken KM, Sausville EL, Girish V, Adebambo OA and Sheltzer JM: Aneuploidy as a promoter and suppressor of malignant growth. Nat Rev Cancer 21: 89-103, 2021.
22. Cao W, Li J, Hao Q, Vadgama JV and Wu Y: AMP-activated protein kinase: A potential therapeutic target for triple-negative breast cancer. Breast Cancer Res 21: 29, 2019.
23. Hadad SM, Baker L, Quinlan PR, Robertson KE, Bray SE, Thomson G, Kellock D, Jordan LB, Purdie CA, Hardie DG, *et al*: Histological evaluation of AMPK signalling in primary breast cancer. BMC Cancer 9: 307, 2009.
24. Mason JM, Wei X, Fletcher GC, Kiarash R, Brokx R, Hodgson R, Beletskaya I, Bray MR, Mak TW, *et al*: Functional characterization of CFI-402257, a potent and selective Mps1/TTK kinase inhibitor, for the treatment of cancer. Proc Natl Acad Sci USA 114: 3127-3132, 2017.
25. Zhang X, Ling Y, Guo Y, Bai Y, Shi X, Gong F, Tan P, Zhang Y, Wei C, He X, *et al*: Mps1 kinase regulates tumor cell viability via its novel role in mitochondria. Cell Death Dis 7: e2292, 2016.
26. Millot C, Millot JM, Morjani H, Desplaces A and Manfait M: Characterization of acidic vesicles in multidrug-resistant and sensitive cancer cells by acridine orange staining and confocal microspectrofluorometry. J Histochem Cytochem 45: 1255-1264, 1997.
27. Chen CY, Chen J, He L and Stiles BL: PTEN: Tumor suppressor and metabolic regulator. Front Endocrinol (Lausanne) 9: 338, 2018.
28. Ippolito MR, Martis V, Hong C, Hong C, Wardenaar R, Zerbib J, Spierings DCJ, Ben-David U, Foijer F and Santaguida S: Aneuploidy-driven genome instability triggers resistance to chemotherapy. Biorxiv: 2020.09.25.313924, 2020.
29. Vasan N, Baselga J and Hyman DM: A view on drug resistance in cancer. Nature 575: 299-309, 2019.
30. Luo J, Solimini NL and Elledge SJ: Principles of cancer therapy: Oncogene and non-oncogene addiction. Cell 136: 823-837, 2009.
31. Manchado E and Malumbres M: Targeting aneuploidy for cancer therapy. Cell 144: 465-466, 2011.
32. Liberti MV and Locasale JW: The warburg effect: How does it benefit cancer cells? Trends Biochem Sci 41: 211-218, 2016.
33. Song IS, Han J and Lee HK: Metformin as an anticancer drug: A commentary on the metabolic determinants of cancer cell sensitivity to glucose limitation and biguanides. J Diabetes Investig 6: 516-518, 2015.
34. Ly P, Kim SB, Kaisani AA, Marian G, Wright WE and Shay JW: Aneuploid human colonic epithelial cells are sensitive to AICAR-induced growth inhibition through EGFR degradation. Oncogene 32: 3139-3146, 2013.
35. Yang L, Li A, Lei Q and Zhang Y: Tumor-intrinsic signaling pathways: Key roles in the regulation of the immunosuppressive tumor microenvironment. J Hematol Oncol 12: 125, 2019.
36. Herriage HC, Huang YT and Calvi BR: The antagonistic relationship between apoptosis and polyploidy in development and cancer. Semin Cell Dev Biol 156: 35-43, 2024.
37. Balko JM, Schwarz LJ, Bhola NE, Kurupi R, Owens P, Miller TW, Gómez H, Cook RS and Arteaga CL: Activation of MAPK pathways due to DUSP4 loss promotes cancer stem cell-like phenotypes in basal-like breast cancer. Cancer Res 73: 6346-6358, 2013.
38. Jeffrey KL, Camps M, Rommel C and Mackay CR: Targeting dual-specificity phosphatases: Manipulating MAP kinase signalling and immune responses. Nat Rev Drug Discov 6: 391-403, 2007.
39. Kuo WL, Duke CJ, Abe MK, Kaplan EL, Gomes S and Rosner MR: ERK7 expression and kinase activity is regulated by the ubiquitin-proteosome pathway. J Biol Chem 279: 23073-23081, 2004.
40. Alkarain A, Jordan R and Slingerland J: p27 deregulation in breast cancer: Prognostic significance and implications for therapy. J Mammary Gland Biol Neoplasia 9: 67-80, 2004.
41. Blain SW, Scher HI, Cordon-Cardo C and Koff A: p27 as a target for cancer therapeutics. Cancer Cell 3: 111-115, 2003.
42. Jhaveri TZ, Woo J, Shang X, Park BH and Gabrielson E: AMP-activated kinase (AMPK) regulates activity of HER2 and EGFR in breast cancer. Oncotarget 6: 14754-14765, 2015.
43. Theodoropoulou S, Brodowska K, Kayama M, Morizane Y, Miller JW, Gragoudas ES and Vavvas DG: Aminoimidazole carboxamide ribonucleotide (AICAR) inhibits the growth of retinoblastoma in vivo by decreasing angiogenesis and inducing apoptosis. PLoS One 8: e52852, 2013.